Intermittent phase synchronization of coupled spatiotemporal chaotic systems

J. Y. Chen,[1] K. W. Wong,[1] H. Y. Zheng,[2] and J. W. Shuai[3]
[1]*Department of Electronic Engineering, City University of Hong Kong, Hong Kong, China*
[2]*Department of Electronic Engineering, Xiamen University, China*
[3]*Department of Biomedical Engineering, Case Western Reserve University, Cleveland, Ohio 44106*
(Received 17 May 2000; published 15 June 2001)

Phase synchronization is studied with a discrete system formed by two coupled map lattices, in which phases are measured in two-dimensional vectors. Simulation results show that by imposing external coupling between the two lattices, phase synchronization can be found in all two-dimensional phase planes between them. When the system is approaching the phase synchronizing state, unstable phase synchronization is observed. This is referred to as intermittent phase synchronization that appears when the trajectories on two interacting phase planes have opposite directions of rotation but with only a small phase difference. The intermittent phase synchronization could also be observed in coupled autonomous systems with diffusive attractors although their phase concepts are inconsistent. Our results show that the intermittent phase synchronization of both discrete and autonomous systems relates to the diffusion or the complexity of the attractors.

DOI: 10.1103/PhysRevE.64.016212 PACS number(s): 05.45.−a, 47.54.+r

I. INTRODUCTION

An interesting and practically significant phenomenon in large ensembles of chaotic maps is the synchronization of connected oscillators [1]. Chaotic synchronization is a fundamental problem in theoretical physics with applications to many areas of science and technology. Various types of synchronization including complete synchronization (CS) [2], lag synchronization [3], and phase synchronization (PS) [4] have been observed.

PS has been studied not only for coupled continuous chaotic systems, but also for the discrete ones. Kaneko [5] considered the phase of discrete systems as ''up'' and ''down'' of data in time series. This phase concept has then attracted recent research interest [6–8]. If two chaotic time series have the same trend of ''up'' and ''down'' movement in the course of iteration, PS is considered to have been achieved [7]. In other papers, the phase is also defined as the local ''maximum'' and ''minimum'' of the time series [8]. A definition of weak PS requires that two series have the same number of local ''maxima'' and ''minima'' over a long period of time, but these turning points are not necessary to occur simultaneously. In order to investigate PS in discrete systems quantitatively, the phase of a discrete system is defined in two-dimensional (2D) phase plane and is distinguished by the rotation direction in the course of iteration [9]. It is shown that the discrete PS phenomena can be applied to symbolic encoding as well as other engineering fields [7,8]. Therefore, it is important to study PS in discrete systems.

From the investigation of coupled map lattices (CMLs), it has been found that phase synchronizing states can emerge in the collective behavior of an ensemble of CMLs as a result of nearest-neighbor [7] or mean field interaction [8]. However, the characteristics of phase difference between two interacting CMLs have not been investigated in detail. In this paper, we will investigate the PS phenomenon in coupled spatiotemporal chaotic systems. Our simulation results show that by imposing a certain external coupling, PS can be found for various pairs of variables between two lattices. Within some coupling regions, unstable PS that exhibits PS characteristics during long intermittent time windows occurs. Therefore it can be considered as *intermittent phase synchronization* (IPS). The mechanism of this phenomenon will be discussed in detail. Furthermore, we use two coupled chaotic oscillators to show that IPS phenomenon could also be found in autonomous chaotic systems with diffusive attractors although the phase concept is inconsistent with that in discrete systems.

This paper is organized as follows. In Sec. II, the basic model of two interacting CMLs is introduced. Moreover, the phase definition for discrete chaotic systems, the criterion for weak PS and the method for calculating the maximum agitation will be stated. With an increase of coupling strength, the phenomena of non-PS, PS, and IPS could be found. Sec. III is devoted to the discussion of IPS. The dynamical analysis of IPS is presented in detail in Sec. IV. Section V briefly describes the IPS in autonomous chaotic systems. Finally, conclusions, are drawn in the last section.

II. BASIC MODEL AND PHASE OF CMLs

In this paper, we will use two CMLs [10], each with length N, to construct a discrete chaotic system for investigating PS. The first lattice is defined as follows:

$$x_i(t+1)=(1-\varepsilon_i-c)f_1(x_i(t))+\varepsilon_i f_1(x_{i+1}(t)) + c[x_i(t)-y_i(t)] \quad (i=1,\ldots,N),$$
$$x_{N+1}(t)=x_1(t), \tag{1}$$

while the second one is

$$y_i(t+1)=(1-\varepsilon_i-c)f_2(y_i(t))+\varepsilon_i f_2(y_{i+1}(t)) + c[y_i(t)-x_i(t)] \quad (i=1,\ldots,N),$$
$$y_{N+1}(t)=y_1(t). \tag{2}$$

Each lattice is called an one-way coupled ring lattice [11]. The parameter c is the interaction between the two CMLs and so it is named the external coupling. The parameter ε_i is the coupling among lattice sites within each CML and is referred to as internal coupling. Moreover, the functions $f_1(x)$ and $f_2(y)$ in the two CMLs can be general one-dimensional discrete chaotic maps.

As the dimension of each CML is N, the number of possible 2D phase planes in each lattice is $N(N-1)/2$. A given plane x_i-x_j (or y_i-y_j) can be represented by (i,j) or a unique number $p_{i,j}$ calculated by

$$P_{i,j}=\frac{(j-1)(j-2)}{2}+i \quad (i<j). \tag{3}$$

Let s_i $(i=1,2)$ be the two variables on a given phase plane. The instantaneous phase on this plane could be defined as [9]

$$\phi(t+1)=\arctan\left(\frac{s_1(t+1)-s_1(t)}{s_2(t+1)-s_2(t)}\right),$$

$$\psi(t)=\phi(t)+2\pi m(t). \tag{4}$$

In order to make the phase increase monotonically in a specific direction, the integer $m(t)$ is chosen as

$$m(t+1)=\begin{cases} m(t+1) & \text{if } \phi(t+1)<\phi(t) \\ m(t) & \text{otherwise,} \end{cases} \tag{5}$$

$t=1,2,3,\ldots$, with $m(1)=0$. Here i is the lattice site, t is the iteration time, and $\psi(t)$ is the phase value.

As the phase of a chaotic system is well defined, one can easily calculate the phase difference $\psi_{i,j[x]}(t)-\psi_{i,j[y]}(t)$ between the corresponding oscillators in 2D phase planes x_i-x_j and y_i-y_j in the two CMLs. If the phase difference does not grow with time and remains bounded, we have a 1:1 phase locking and generally

$$|\psi_{i,j[x]}(t)-\psi_{i,j[y]}(t)|<(\text{const})_{i,j}. \tag{6}$$

We observe that small values of $(\text{const})_{i,j}$ indicate strong PS states. In order to facilitate the investigation of the strength of PS, $\delta_{i,j}$ is set as the maximum value of $|\psi_{i,j[x]}(t)-\psi_{i,j[y]}(t)|$ at any iteration from 1 to T (where $T\to\infty$). By this means, the phase locking states can be characterized by $\delta_{i,j}$ directly. The phase states can also be reflected by the mean frequency defined as [12]

$$\omega_{i,j}=\langle\dot{\phi}_{i,j}\rangle=\lim_{\tau\to\infty}\frac{\psi_{i,j}(T)-\psi_{i,j}(0)}{T}. \tag{7}$$

PS is achieved when the frequency difference $|\omega_{i,j}(x)-\omega_{i,j}(y)|=\Delta\omega_{i,j}\to 0$.

The two CMLs may achieve complete synchronization with a certain external coupling, even when the start points are different. Complete synchronization means that $x_i(t)=y_i(t)$. Therefore, the mean absolute amplitude difference of the two CMLs is given by

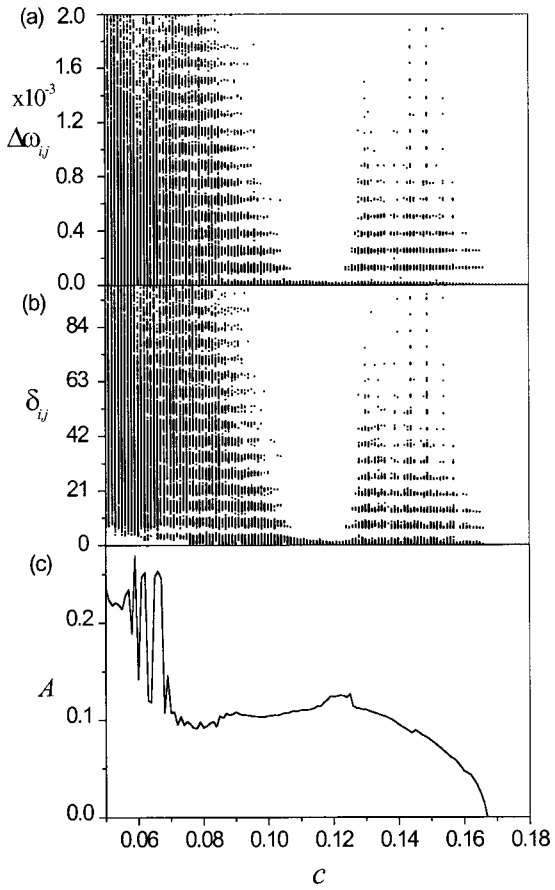

FIG. 1. A plot of (a) the frequency difference $\Delta\omega_{i,j}$, (b) the maximum agitation of phase difference $\delta_{i,j}$, and (c) the mean absolute amplitude difference A vs the external coupling c in the range $0.05<c<0.18$. In (a) and (b), one dot represents each (i,j) plane.

$$A=\lim_{\tau\to\infty}\frac{1}{T}\sum_{r=1}^{T}\left(\frac{1}{N}\sum_{i=1}^{N}|x_i-y_i|\right) \tag{8}$$

This parameter can be used to detect whether the phase planes in concern exhibit complete synchronization or not.

Let the two functions in Eqs. (1) and (2) be logistic maps with different initial conditions, i.e., $f_1(x)=\mu_1 x(1-x)$ and $f_2(y)=\mu_2 y(1-y)$. If not specified, the parameters chosen are $\mu_1=\mu_2=4$ and $\varepsilon_i=0.1+(0.1/N)(i-1)$, where $i=1,\ldots,N$ and $N=50$. This implies that Eqs. (1) and (2) are two identical CMLs and the internal coupling ε_i ranges from 0.1 to 0.2 at equal intervals. The different values of ε_i facilitate the identification of the lattice site i from others. All the simulation results reported here are obtained from a total of $T=5\times10^4$ iterations, with the first 1×10^4 transient iterations omitted.

The simulation results correspond to $0.05\leqslant c\leqslant 0.18$ are shown in Figs. 1(a) and 1(b). With an increase of external coupling, $\Delta\omega_{i,j}$ as well as $\delta_{i,j}$ are found to have obvious jumps referred to as IPS that may help in developing new features of phase synchronization in discrete chaotic systems. When $c>0.107$, IPS vanishes and PS is obtained. Furthermore, when $c>0.125$, PS on some of the phase planes is

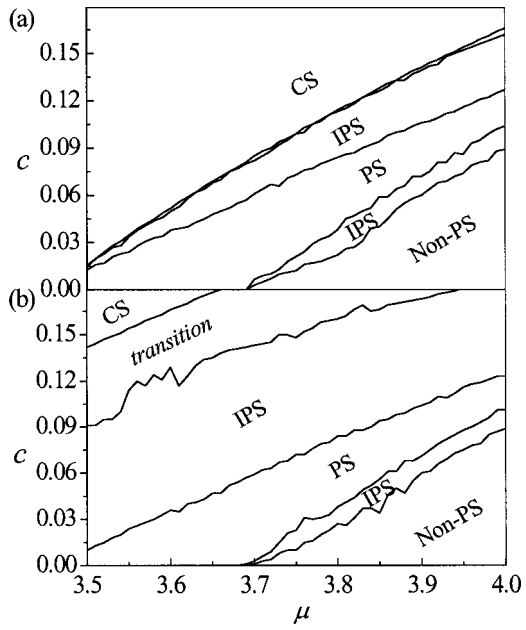

FIG. 2. Phase diagram of Eqs. (1) and (2): The parameter μ changes from 3.5 to 4.0 in steps of 0.01. The regions correspond to non-phase synchronization (non-PS), intermittent phase synchronization (IPS), phase synchronization (PS), and complete synchronization (CS) are marked accordingly. The area between the IPS and CS regions is the transition band. (a) Identical CMLs with parameters $\mu_1=\mu_2=\mu$. (b) Nonidentical CMLs with parameters $\mu_1=\mu$ and $\mu_2=\mu-0.01$.

destroyed by a jumping feature and the system enters IPS again. As c approaches 0.178, $A=0$ and the two lattices are in complete synchronization.

The IPS phenomenon at various parameter values is generated and shown in Fig. 2(a). When the parameter μ ($\mu_1=\mu_2=\mu$) varies from 3.5 to 4.0, some regions corresponding to IPS are found to have a long band shape. This shows that IPS can be found at various parameter values. The narrow region between the IPS and CS regions is the transition band. Details of Fig. 2(b) as well as the dynamics that cause IPS will be discussed in Sec. IV.

III. INTERMITTENT PHASE SYNCHRONIZATION (IPS)

The jumping phenomenon occurred in the frequency difference $\Delta\omega_{i,j}$ and the maximum agitation $\delta_{i,j}$ is a characteristic of discrete interconnected chaotic systems. In order to analyze this feature in detail, some further simulations are performed and their results are shown in Figs. 3(a) and 3(b). From these figures, there are several layers of points found at IPS. For convenience, we label the layers as $L(k)(k=1,2,3,\ldots)$ from bottom to top. Only the four bottom layers are shown in Fig. 3(b). The dashed lines mark the $k\pi$ levels. The jumping phenomenon found in Fig. 3(a) is mainly caused by the jumping agitation shown in Fig. 3(b). The maximum agitation is directly related to the strength of PS or non-PS. Basically, when $\Delta\omega_{i,j}\to 0$ (corresponding to PS), the corresponding $\delta_{i,j}$ may distribute in all layers. In particular, phase locking (maximum agitation under PS) in

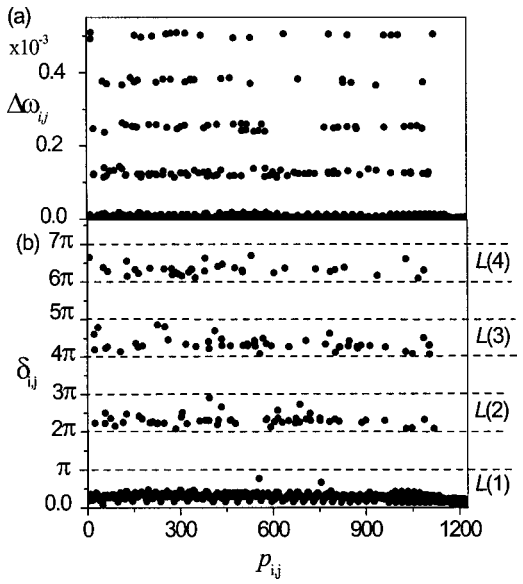

FIG. 3. A plot of (a) the frequency difference $\Delta\omega_{i,j}$, (b) the maximum agitation of phase difference $\delta_{i,j}$ on each phase plane $p_{i,j}$, (only the four bottom layers are shown). The external coupling is $c=0.13$ while the parameters are $\mu_1=\mu_2=4$.

the same layer shows approximately the same strength of PS. Moreover, lower layers correspond to a stronger PS than upper ones. For the nonsynchronization region where $\Delta\omega_{i,j}>0$, the corresponding $\delta_{i,j}$ has a distribution of values from $L(2)$ to upper layers. For example, in $L(2)$, the largest value of the frequency difference allowed is $\Delta\omega_{i,j}<3\pi/T\approx 1.8\times 10^{-3}$ within our time scale of simulations. The nonsynchronization planes whose $\delta_{i,j}$ locate in $L(2)$ correspond to the state closest to PS. However, the corresponding $\Delta\omega_{i,j}>0$ and so it can only be considered as non-PS according to Eq. (7). The jumping phenomenon in the non-PS region closest to weak PS is interesting. Its strength needs to be measured. As a result, it is termed the IPS state.

IPS can be described as

$$\omega'_{i,j}=\langle\dot{\phi}_{i,j}\rangle_{\Delta T}=\frac{\phi_{i,j}(T_2)-\phi_{i,j}(T_1)}{\Delta T}$$

and

$$|\omega'_{i,j}(x)-\omega'_{i,j}(y)|=\Delta\omega'_{i,j}\to 0, \tag{9}$$

where $\Delta T=T_2-T_1$ is the long time window named laminar length. This term replaces $T\to\infty$ in Eq. (7). Here, the laminar length is the time elapsed between two successive 2π jumps [13]. If the two phase planes are in a nonsynchronized state ($\Delta\omega_{i,j}>0$) when $T\to\infty$, but occasionally show $\Delta\omega'_{i,j}\to 0$ during different intervals ΔT, their relation can be considered as IPS when ΔT is very large. This kind of 2π jump is more likely to be the result of unstable PS. The phase difference can be considered as locked during most of the long iteration, but bursts 2π intermittently.

The difference between non-PS and IPS is illustrated in Figs. 4(a)–4(c), which show the phase difference in the course of iteration on three phase planes (30, 42), (23, 49),

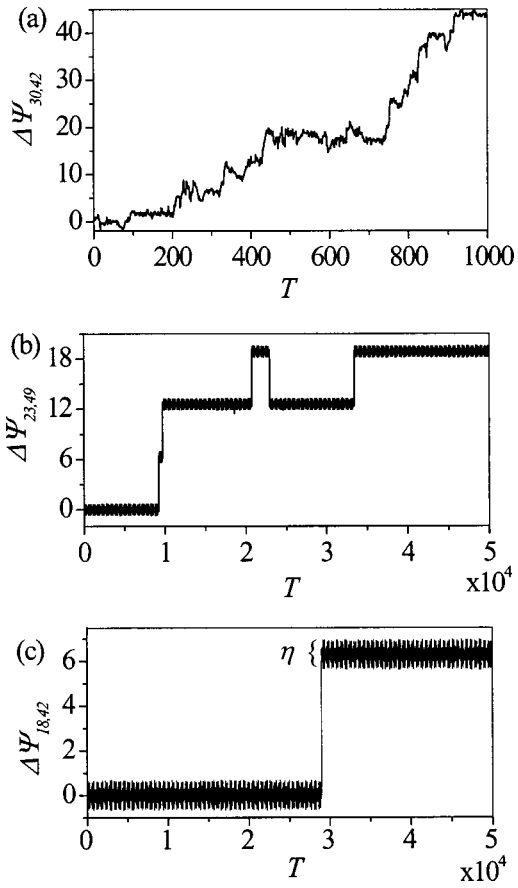

FIG. 4. A plot of the phase difference vs iterating time on different planes of two CMLs at various external coupling c and $\mu_1=\mu_2=4$. (a) plane (30, 42) with external coupling $c=0.05$; (b) plane (23, 49) and (c) plane (18, 42) with $c=0.13$. In (c), η is the agitation in one laminar length.

and (18, 42), respectively. Figure 4(a) corresponds to the external coupling $c=0.05$. There are no $n\pi$ jumps as in Figs. 1(a) and 1(b). The phase difference increases irregularly. While Figs. 4(b) and 4(c) are the simulation results of IPS for $c=0.13$, their $\delta_{i,j}$ are respectively in the $L(2)$ and $L(4)$ bands marked in Fig. 3(b). We find that the laminar length can be very large. For example, the two PS windows in Fig. 4(c) have durations of 28 966 and 21 034, respectively.

IV. DYNAMICAL ANALYSIS

In this section, we first develop a simple method to measure the IPS. According to Fig. 3(b), suppose that $p(L(i))$ is the number of phase planes distributed in the region $L(i)$. We now define the IPS ratio α as

$$\alpha=\frac{2}{N(N-1)}\sum_{i=1}^{\infty} p(L(i)). \tag{10}$$

Evidently, the PS ratio β corresponds to the special case that only the first region $L(1)$ is considered is given by

$$\beta=\frac{2}{N(N-1)}p(L(1)). \tag{11}$$

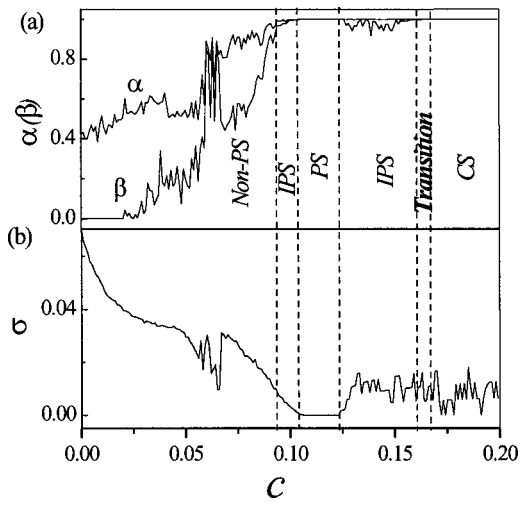

FIG. 5. A plot of (a) the IPS ratio α and PS ratio β; (b) the average abnormal ratio σ. The area between the IPS and CS regions is the transition band. The external coupling strength c varies from 0.0 to 0.2.

When $\alpha=\beta\approx 1$ and their corresponding amplitudes are nearly independent, the system is in PS. On the other hand, if $\alpha\approx 1$ and $\beta<1$, it is in IPS. Note that this method could only reflect the relationship between IPS and PS approximately. The reason is that from the above analysis, several dots in $L(i)$ (where $i>1$ and $\Delta\omega_{i,j}\to 0$) also belong to PS although the synchronization is weak. As we do not care about the exact value of α and β, and the synchronizing states are only measured statistically, the simple approximate method is always effective in analysis. By this means, the phenomena of Fig. 1(b) could be described by the curves of α and β shown in Fig. 5(a).

On the other hand, different properties such as PS and IPS could be found at different external coupling strengths. It is important to uncover the dynamical mechanism behind them. The direction of iteration may help in this. In order to characterize the transitions quantitatively, we represent the direction of iteration in every unit of lattices (i.e., ''up'' or ''down'') as binary symbols (i.e., ''1'' or ''0''). If the binary symbols of one unit are 10101010 . . . at $t=1,2,3\ldots$, the chaotic behavior is changed regularly and is considered as simple chaos. However, if the binary symbols show 011101001, the output is complex chaos [7]. We will show that IPS corresponds to a relatively weak complex chaos and PS always corresponds to simple chaos. Here, we only show the analysis for Eq. (1). The corresponding calculation using Eq. (2) is the same. The quantitative characterization of the ith unit at some time t is shown as follows [7]:

$$\gamma_i^x(t)=\begin{cases}1, & \text{if } x_i(t)/x_i(t-1)>1,\\ 0, & \text{otherwise,}\end{cases} \tag{12}$$

where $\gamma_i^x(t)$ is named the phase series. An average abnormal ratio σ^x could measure the strength of complexity [7]:

$$\sigma^x=\frac{1}{T}\sum_{i=0}^{T}\frac{1}{N}\sum_{i=1}^{N}\sigma_i^x(t),$$

where

$$\sigma_i^x(t)=\begin{cases}1, & \text{if } \gamma_i(t)=\gamma_i(t-1)\\ 0, & \text{otherwise.}\end{cases}$$

Then

$$\sigma=(\sigma^x+\sigma^y)/2, \tag{13}$$

where σ^y is the average abnormal ratio of Eq. (2) and σ is the corresponding mean value between Eqs. (1) and (2). We take a simple example to show the relationship between $\gamma_i(t)$ and $\sigma_i(t)$. If the binary series of the ith unit read $101011001\cdots$, $\sigma_i(t)$ becomes $00001010\cdots$. Hence, the chaotic behavior in the iterated systems will be denoted as simple chaos if $\sigma=0$. It is classified as complex chaos if $\sigma>0$ [7]. Figure 5(b) shows the temporal evolution of the average abnormal ratio with the increase of external coupling strength. When $\sigma=0$, it corresponds to PS region. While the value of σ agitates round 0.01 approximately, IPS phenomenon is observed in the dynamics. If $\sigma>0.02$, it is the non-PS region. In this regard, the IPS always corresponds to weak complex chaos. In CS region, although the abnormal ratio keeps strong agitation and the weak complex chaos still appears, the strong external coupling pushes the two CMLs to CS. In Fig. 5, the area between regions IPS and CS shows PS phenomenon. However, as this narrow region corresponds to the rapid reduction of the average amplitudes shown in Fig. 1(c), it belongs to a strong correlation of interacting amplitudes. Thus, it could be considered as transition region from IPS to CS.

In a single unit of the lattice, the simple chaos in PS region indicates that the unit regularly changes between ''up'' and ''down.'' No two successive ''up'' or ''down'' movements exist. This mechanism facilitates to form two regions divided by a narrow gap in pattern of temporal evolution of the unit's iterations. The trajectory of each map splits into two regions as shown in Fig. 6(a). The field between these two regions becomes a broad gap shown with two dotted lines. The gap size is about 0.1.

The pattern of temporal evolution includes a large gap size that can be utilized for encoding [14]. For example, we can define a binary partition $S(n)$ in phase space with elements $S(n)=1$ when x_i is located in the upper region (i.e., >0.75) or -1 when x_i is located in the lower region (i.e., <0.65). The trajectory is encoded according to which partition a point is in. Moreover, the large gap size indicates that the model will have high noise resistance using communication with chaos techniques. This advantage is important in communication. Such a symbolic encoding may be applicable to dynamic systems and can be discussed using information theory [15].

The IPS state corresponds to weak complexity of chaos. In most cases, the unit regularly changes with ''up'' and ''down.'' However, in some cases, two or more successive ''up'' or ''down'' occurs. Therefore, the pattern of temporal evolution always appears to have blurry gaps as is shown in Fig. 6(b). At non-PS state, the relatively strong complexity

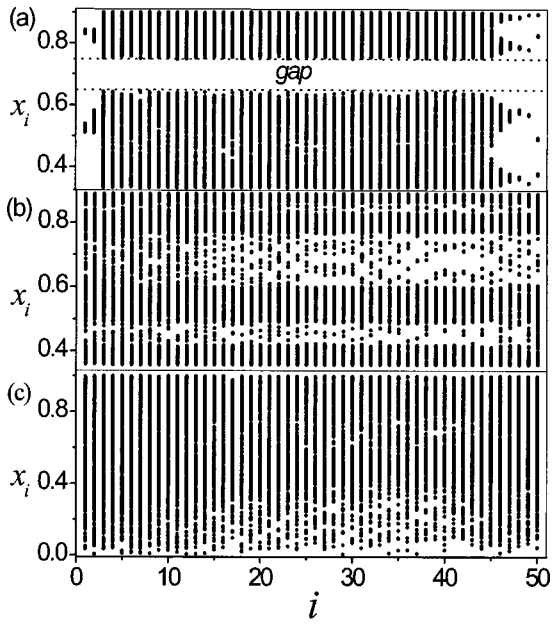

FIG. 6. Pattern of temporal evolution of x_i with 400 iteration dots. (a) $c=0.12$. (b) IPS state with $c=0.13$ and (c) non-PS state with $c=0$.

of chaos causes a disorder of the ''up'' and ''down'' changes. Thus the narrow gap disappears. This is shown in Fig. 6(c).

The above analysis is based on the identical coupling systems represented by Eqs. (1) and (2). However, in practical systems, we cannot make all the units identical. Therefore, one may ask what would the output be if Eqs. (1) and (2) are not identical? To explore this, we investigate the PS and IPS states with a tiny difference between the value of μ_1 and μ_2. Let $\mu_1=\mu$ and $\mu_2=\mu-0.01$. The simulation results with various μ and c are shown in Fig. 2(b). When it is compared with Fig. 2(a), a significant difference is observed, i.e., the IPS region is extended evidently. The little difference between the two lattices may be regarded as an effective noise term that increases the degree of disorder in the iterating direction. By this means, the consideration of IPS should not be ignored in practical applications.

This kind of IPS phenomenon may be explained by the mechanism that two phases run into a region where a small shift of phase difference leads to the opposite rotation directions of the trajectory in the two interacting phase planes. This is shown graphically in Figs. 7(a) and 7(b). The vectors $X=(x_i,x_j)$ and $Y=(y_i,y_j)$ are the corresponding vectors in the two interacting CMLs. The dashed vectors $X'(t+1)-X(t-1)$ and $Y'(t+1)-Y(t-1)$ are in parallel with the two solid vectors $X(t+1)-X(t)$ and $Y(t+1)-Y(t)$. Moreover, θ_x is the phase between $X(t)-X(t-1)$ and $X(t+1)-X(t)$ while θ_y is that between $Y(t)-Y(t-1)$ and $Y(t+1)-Y(t)$. Assume that the two systems have the same phase at time t, but possess a nonzero phase difference at time $t+1$. When compared to $X(t)-X(t-1)$ and $Y(t)-Y(t-1)$, respectively, $X(t+1)-X(t)$ moves in clockwise rotation while $Y(t+1)-Y(t)$ is in counterclockwise rotation. If the agitation $|\theta_x-\theta_y|<\eta$ [where the value of η is

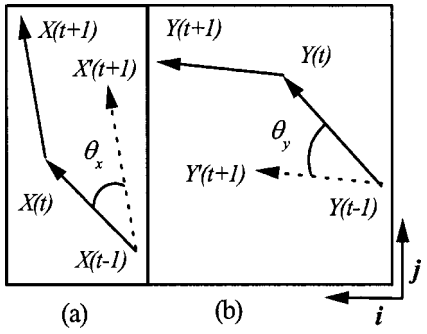

FIG. 7. Schematic diagrams showing the region with opposite direction of rotation on the phase plane (i,j) of the two CMLs. (a) the vector $X=(x_i,x_j)$ given by Eq. (1). (b) the vector $Y=(y_i,y_j)$ given by Eq. (2). The dashed vectors $X'(t+1)-X(t-1)$ and $Y'(t+1)-Y(t-1)$ are in parallel with the two solid vectors $X(t+1)-X(t)$ and $Y(t+1)-Y(t)$.

shown in Fig. 4(c)], the two trajectories appear similar at time $t+1$. However, as the phase increases in the same direction of rotation monotonously [9] according to Eq. (5), it is found that the phase in Fig. 7(a) is not θ_x at time $t+1$, but $2\pi-\theta_x$. This corresponds to a jump of approximately 2π.

It is evident that when two systems encounter the situation shown in Figs. 7(a) and 7(b), there may be a phase jump of 2π. Under the same condition, if the trajectory of the phase planes never faces this situation, the planes can easily maintain PS with a certain external coupling. To summarize, IPS is referred to as the situation that two trajectories have similar rotation but in some cases with phase shift in opposite directions. The phase difference is then unstable and may have 2π jumps intermittently.

V. IPS IN AUTONOMOUS CHAOTIC SYSTEMS

Although the phase concepts between autonomous and discrete systems are inconsistent, IPS phenomenon could also be found in autonomous chaotic systems. For coherent attractors, when the coupling strength is approaching phase transition, 2π phase jumps could be found before phase transition and the average laminar length becomes longer. When this length is so long that no period could be found, this kind of phase slips is considered as IPS [16]. However, as the attractors are coherent, the IPS region is very narrow. When the attractors become diffused, such as inducing external noise [17] to coherent attractors or using diffusive attractors [13] directly, IPS could occur with a relative large range of coupling strength.

In this section, we take two coupled diffusive oscillators, such as funnel attractors [12], as an example to show the IPS between them. The model equation is written as [18]

$$\dot{x}_{1,2}=-\omega_{1,2}y_{1,2}-z_{1,2}+\varepsilon(x_{2,1}-x_{1,2}),$$

$$\dot{y}_{1,2}=\omega_{1,2}x_{,2}+0.22y_{1,2}, \qquad (14)$$

$$\dot{z}_{1,2}=0.1+z_{1,2}(x_{1,2}-8.5),$$

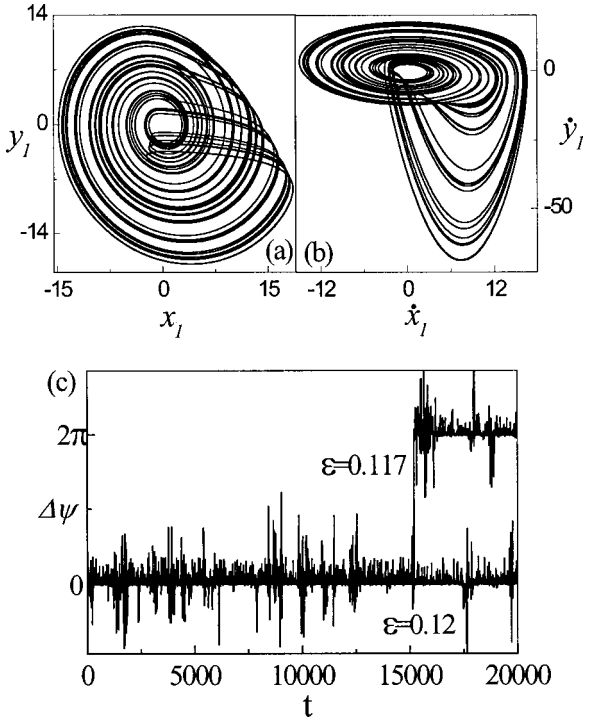

FIG. 8. Projections of phase portraits and phase difference of the two coupled Rössler oscillators. (a) Funnel attractor in (x_1,y_1)-plane at $\varepsilon=0$. (b) Funnel attractor of (a) in $(\dot{x}_1,\dot{y}_1)$-plane. It possesses a rotation center at (0,0). The attractor in (x_2,y_2)-plane has similar properties and is not shown here. (c) Time series of phase difference $\Delta\psi$ in two coupled oscillators at various values of ε. When $\varepsilon=0.117$, it shows IPS phenomenon. PS seems to have achieved for the observed time scale when $\varepsilon=0.12$.

where the natural frequencies are $\omega_1=0.98$ and $\omega_2=0.99$, ε is the coupling strength for the interaction of the two oscillators.

As observed from Fig. 8(a), both the attractors in Eq. (14) are funnel. In most cases, a trajectory makes a trip around the origin in the (x_1,y_1)-plane. However, sometimes it makes only a half of this round trip. These irregular phase shifts can be interpreted as an effective noise that breaks the phase coherence [12]. As the trajectory has only a small number of irregular phase shifts, the attractor is considered as a diffusive but relatively weak one.

To investigate the properties of funnel attractors, a major difficulty is to obtain the instantaneous phase. Due to this limit, the properties of funnel attractors were always uncovered by indirect methods such as the statistical method [12]. The disadvantage is that only macroscopical properties can be found. In the following, we introduce a method to obtain the instantaneous phase. Then we describe the IPS phenomenon near the PS transition. The instantaneous phase ψ could be obtained by [19]

$$\psi=\arctan\left(\frac{\dot{x}(t)}{\dot{y}(t)}\right). \qquad (15)$$

Equation (15) is suitable for funnel attractors whose trajectory has only a single rotation direction. As Eq. (14) pos-

sesses the kind of funnel attractors shown in Fig. 8(a), we can use it to obtain the instantaneous phase. Evidently, the new $(\dot{x}_1,\dot{y}_1)$-plane should contain an attractor with rotation center at (0, 0) as shown in Fig. 8(b). With the aid of Eq. (15), the IPS phenomenon could be explicitly found in Fig. 8(c) at $\varepsilon=0.117$. While at $\varepsilon=0.12$, it is considered as PS within our time scale of simulations. The average laminar length increases exponentially when ε approaches PS transition [13,16,17]. However, if the diffusion is too strong, such as strong funnel attractors [12] or coherent attractors with large mismatch of parameters [20], PS as well as IPS may not appear.

VI. CONCLUSION

In conclusion, the characteristics of PS between two CMLs are studied extensively. With an external coupling, PS in all 2D phase planes can be obtained. In the route from non-PS to PS, the maximum agitation always exhibits the $n\pi$ jump phenomenon. In some particular external coupling, the phase difference can appear to be IPS that is caused by the situation where a small shift of phase makes the two trajectories rotate in opposite directions. This phenomenon could also be described by weak complex chaos. The PS phenomenon caused by simple chaos may be applied to symbolic encoding with strong noise resistance in communication while the investigation of IPS may lead to potential applications in engineering control and pattern formation. Furthermore, we demonstrate that the IPS could also be found in autonomous chaotic systems with diffusive attractors. Thus, although the phase concepts between discrete and autonomous systems are inconsistent, IPS for both of them relates to the diffusion or complexity of attractors.

ACKNOWLEDGMENTS

We thank P. J. Hahn for a careful reading and revision of the manuscript. The work described in this paper was fully supported by a grant from CityU (Project No. 7001077).

[1] P. C. Matthews and S. H. Strogatz, Phys. Rev. Lett. **65**, 1701 (1990); M. D. S. Vieira, A. J. Lichtenberg, and M. A. Lieberman, Int. J. Bifurcation Chaos Appl. Sci. Eng. **4**, 1563 (1994).

[2] J. Y. Chen, K. W. Wong, and J. W. Shuai, Phys. Lett. A **263**, 315 (1999); J. H. Peng, E. J. Ding, M. Ding, and W. Yang, Phys. Rev. Lett. **76**, 904 (1996); Y. Liu and P. Davis, Phys. Rev. E **61**, 2176 (2000); Z. Liu, S. Chen, and B. Hu, *ibid.* **59**, 2187 (1999).

[3] M. G. Rosenblum, A. S. Pikovsky, and J. Kurths, Phys. Rev. Lett. **78**, 4193 (1998).

[4] M. G. Rosenblum, A. S. Pikovsky, and J. Kurths, Phys. Rev. Lett. **76**, 1804 (1996); S. Boccaletti, J. Bragard, F. T. Arecchi, and H. Mancinil, *ibid.* **83**, 536 (1999); C. Schader, M. G. Rosenblum, J. Kurths, and H. Abel, Nature (London) **392**, 239 (1998); B. Blasius, A. Huppert, and L. Stone, *ibid.* **399**, 354 (1999); I. Kim, C. M. Kim, W. H. Kye, and Y. J. Park, Phys. Rev. E **62**, 8826 (2000).

[5] K. Kaneko, Phys. Rev. Lett. **63**, 219 (1989); Physica D **41**, 137 (1990).

[6] H. Fujigaki and T. Shimada, Phys. Rev. E **55**, 2426 (1997).

[7] B. Hu and Z. Liu, Phys. Rev. E **62**, 2114 (2000); W. Wang, Z. Liu, and B. Hu, Phys. Rev. Lett. **84**, 2610 (2000).

[8] F. S. de San Roman, S. Boccaletti, D. Maza, and H. Mancini, Phys. Rev. Lett. **81**, 3639 (1998); D. Maza, S. Boccaletti, and H. Mancini, Int. J. Bifurcation Chaos Appl. Sci. Eng. **10**, 829 (2000).

[9] J. Y. Chen, K. W. Wong, Z. X. Chen, S. C. Xu, and J. W. Shuai, Phys. Rev. E **61**, 2559 (2000).

[10] T. Bohr and O. B. Christensen, Phys. Rev. Lett. **63**, 2161 (1989).

[11] L. H. Xiao, G. Hu, and Z. Qu, Phys. Rev. Lett. **77**, 4162 (1996).

[12] G. V. Osipov, A. S. Pikovsky, M. G. Rosenblum, and J. Kurths, Phys. Rev. E **55**, 2353 (1997); A. S. Pikovsky, M. G. Rosenblum, and J. Kurths, Europhys. Lett. **34**, 165 (1996).

[13] I. Kim, C. M. Kim, W. H. Kye, and Y. J. Park, Phys. Rev. E **62**, 8826 (2000).

[14] E. Bollt, Y. C. Lai, and C. Grebogi, Phys. Rev. Lett. **79**, 3787 (1997).

[15] C. Shannon and W. Wwaver, *The Mathematical Theory of Communication* (University of Illinois Press, Urbana, IL, 1949).

[16] K. J. Lee, Y. Kwak, and T. K. Lim, Phys. Rev. Lett. **81**, 321 (1998); E. Rosa, Jr., E. Ott, and M. H. Hess, *ibid.* **80**, 1642 (1998).

[17] V. Andrade, R. L. Davidchack, and Y. C. Lai, Phys. Rev. E **61**, 3230 (2000); W. H. Kye and C. M. Kim, *ibid.* **62**, 6304 (2000).

[18] O. E. Rössler, Phys. Lett. **57A**, 397 (1976).

[19] J. Y. Chen, K. W. Wong, and J. W. Shuai (unpublished).

[20] Z. G. Zheng and G. Hu, Phys. Rev. E **62**, 7882 (2000).